

Estimation of Ear Parameters Applicable to Otoplasty Surgery

Ali Fahmi Jafargholkhanloo¹, Mousa Shamsi^{2*}

1- Biomedical Engineering, Sahand University of Technology, Tabriz, Iran.

2*- Biomedical Engineering, Sahand University of Technology, Tabriz, Iran.

¹a_fahmi@sut.ac.ir, ^{2*}Shamsi@sut.ac.ir

Corresponding author address: Mousa Shamsi, Faculty of Biomedical Engineering, Sahand University of Technology, Tabriz, Iran, Post Code:

Abstract- Analysis of facial color images is very important as a result of its numerous applications in facial surgeries. The development of different tools in the field of facial surgery analysis has helped surgeons before and after surgery. In this article, an Active Contour Model (ACM) based on Local Gaussian Distribution Fitting (LGDF) is introduced for the contour extraction of the ear area. The LGDF model is a region-based method in the Active Contour Model that unlike other models such as the Chan-Vese is not sensitive to intensity inhomogeneity of the image. After the contour extraction of the ear area, in the second step, with the four landmarks detection, ear parameters containing: length, width and external angle of ear were measured for analysis in the Otoplasty surgery. The proposed algorithm was evaluated on the AMI and Sahand University of Technology (SUT) databases. The proposed algorithm has an accuracy of %96.432, %97.423 and %85.546 in the AMI database and an accuracy of %98.381, %97.237 and %87.864 in the SUT database for the length, width and external angle of the ear parameters, respectively.

Keywords- Active Contour Model, Color Images Analysis, Analysis of Ear Anthropometry, Facial Surgery Analysis, Otoplasty Surgery.

I. INTRODUCTION

The significance of human facial images analysis has increased considerably as a result of its numerous applications, such as in facial surgery. The human face plays a very important role in the appearance of the person. Even the slightest deformation in the human face can have a marked effect on the appearance of the person's face [1]. Otoplasty surgery is a method that changes the size and shape of ears. In this surgical procedure, the abnormal structure of the ear, that has been congenital during growth or due to accidents, can be modified. Actually, it can be said that the results of Otoplasty are strongly influenced by the surgeon's analysis [2,3]. Many people have had problems with their ear size and its appearance since childhood; either, the bulge of their ears are not symmetrical or there is too much prolapse in their ears. As a result, the main aim of an Otoplasty surgeon is to reestablish the natural appearance of the auricle and the relationship between the auricle and the head [4]. In Otoplasty surgery, if the ears are bulging, they could be

modified by stitching the cartilage and bringing them closer to the head. If one of the ears is higher than the other one, they could be symmetrically adjusted through Otoplasty surgery [5]. From the perspective of beauty, a normal ear is about 20 degrees to the vertical line. The ears of adults have a length of about 50 to 60 mm and width of about 55% of its length, Fig. 1. The progress in the applications of computers and image processing software has facilitated the work of plastic surgeons, and has opened a new outlook for them in terms of data acquisition before operation [6]. Ears are among the important parts of the face and play a very important role in facial beauty. People who are dissatisfied with the size and protuberance of their ears can change its appearance by Otoplasty surgery. Otoplasty surgery modifies the ear cartilage tissue and corrects important problems regarding concave and convex ear structure [7-9]. Ear anthropometric measurement is one of the important tasks performed by most surgeons before surgery, to improve the quality of the Otoplasty surgery. The important ear anthropometrics include: length, width and the external angle of the ear.

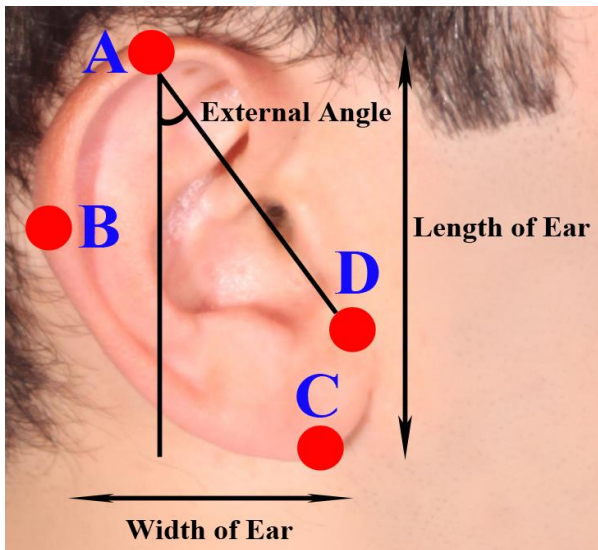


Fig. 1. Normal ear parameters and view of three landmarks in the ear. (A) The superior point of the helical rim. (B) The midpoint of helix. (C) Auricle. (D) lobule.

Nowadays, the facial surgery and aesthetic analysis in the field of digital image processing and computer vision has been interested for researchers. There are few articles in the facial surgery analysis for facial anthropometric measurement. The most important part of the proposed algorithm is the ear contour extraction. In order to performance comparison of the proposed algorithm with other methods used in the digital image processing and computer vision, we will briefly review the ear contour extraction methods. In order to perform ear contour extraction in [10], at first, the landmarks were selected manually and using the active contour model, the ear's external contour is extracted. Finally, Canny Edge Detector (CED) was used to extract the ear inner contour. In [11], to determine the ear curvature, first, the median filter is used to remove the noise. Finally, the filtered image is used for canny edge detector. In [12], in order to perform ear contour extraction as well as determine the minimum and maximum points, the Canny edge detector and image geometric features were used. Ajay et al. [13], presented a Fourier descriptor to ear contour extraction. In this method, a histogram equalization was used to normalize the image. After normalization, morphological operators were used to opening and closing the image. For ear contour extraction, the output of the morphological operator is multiplied in the produced mask. Finally, ear contour extraction was used as a Fourier descriptor. In [14], a method has been presented for ear segmentation. The likelihood image method is used for skin detection. Finally, using the suitable threshold and morphological operators the ear contour was extracted. In [15], a novel method has been presented for ear verification based on the features extracted using a bank of filters learnt using Topographic Locally Competitive Algorithm (TLCA). In this study, it has been presented a new scheme to detect both deformed and surgically altered ear using one-class classification. Extensive experiments have been performed on both normal and surgically altered ear database. In [16], a

camera identification algorithm has been presented for ear biometric images using tunable filter banks as a feature extractor. In this study, features have been extracted using filter bank, based on a half-band polynomial of 14th order. The ear image has been divided into six parts. Wavelet based on tunable filter bank has been applied to each block. Features from each block has been extracted in terms of energy function. In [17], an efficient ear pattern sensor by introducing a new imaging technique has been presented that is capable of simultaneous retrieval of the topographic details and its liveliness information. In this study, a collimated laser beam has been made incident on a sinusoidal grating, and the resultant structured pattern has been projected towards the ear specimen. As well as, time series bio-speckled fringe sequences have been recorded using a CCD camera for detection of topographic information and liveliness. For noise removal, a combination of windowed Fourier filtering and low pass filtering has been used.

Generally, in an Otoplasty operation, surgeons need visual information about the ear and surrounding areas, such as precise biometrics of length, width and external angle of the ear. This study has proposed a method which assists Otoplasty surgeons in measuring important parameters in the ear area, such as the mentioned above parameters. For this purpose, an active contour model was introduced based on the local Gaussian distribution algorithm. This paper is organized as follows: in Section 2 the active contour model is explained based on LGDF. Section 3 presents an explanation on how we can extract key points of the ear area, in order to measure important parameters of the ear for Otoplasty surgery analysis. In Section 4 the experimental results are explained, and finally, in Section 5 the results are discussed.

II. LOCAL GAUSSIAN DISTRIBUTION FITTING

As shown in Fig. 2, the proposed algorithm is divided into three sections including preprocessing, LGDF model and feature extraction. First, we introduce the LGDF model, then we describe the preprocessing and landmark detection in the next section.

The active contour model based on LGDF is proper for the segmentation of images that have a non-uniform spatial intensity. In this model, the spatial intensities of images could be described by using the Gaussian distribution with different mean and variances. In this model, an energy fitting of local Gaussian distribution is defined as variables including a level set function, mean, and local variances. In the LGDF model, the level set function is designed as a gradient flow and it could minimize the energy function and cause the movement of zero-level function to the desired locations [18,19].

It was assumed that Ω is a set of discrete regions in an image, Ω , with N number of regions. In this case, the two general conditions for segmentation of an image, are as follows [20]:

$$\left\{ \begin{array}{l} \Omega = \cup_{i=1}^N \Omega_i \\ \Omega_i \cap \Omega_j \neq \phi \text{ for } i \neq j \end{array} \right\}$$

If for any point of X in the image, we define a circular

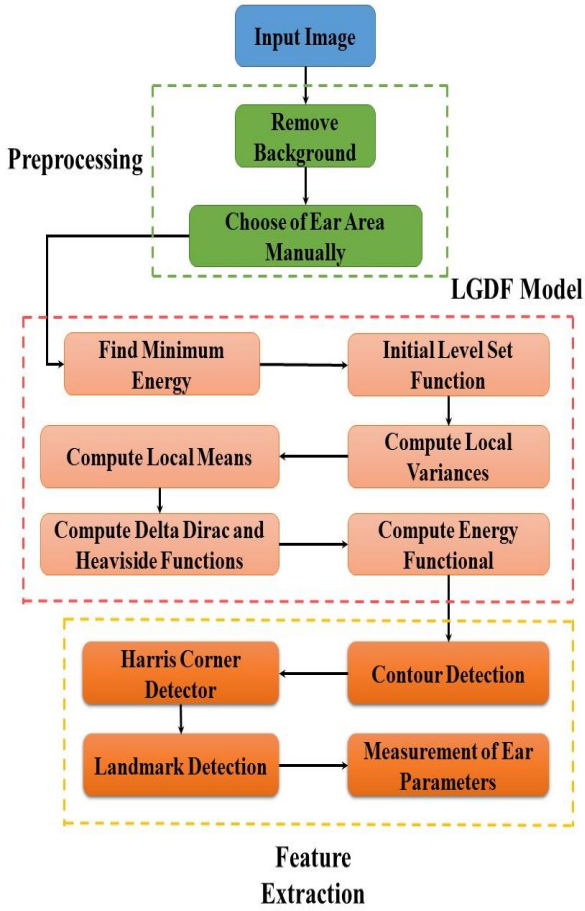


Fig. 2. Block diagram of the proposed algorithm for measuring the important ear parameters.

neighborhood of a small radius ρ as follows:

$$\vartheta_x \triangleq \{y: |x - y| \leq \rho\} \quad (2)$$

Based on Bayes rule, that posterior probability of the sub regions will be defined as follows:

$$p(y \in \Omega_i \cap \vartheta_x | I(y)) = \frac{p(I(y) | y \in \Omega_i \cap \vartheta_x) p(y \in \Omega_i \cap \vartheta_x)}{p(I(y))} \quad (3)$$

Assuming that the pixels within any region are independent, then the maximum will only be obtained if the following statement is maximized:

$$\prod_{i=1}^N \prod_{y \in \Omega_i \cap \vartheta_x} p_{i,x}(I(y)) \quad (4)$$

$$E_x^{LGDF} = \sum_{i=1}^N \int_{\Omega_i \cap \vartheta_x} -\log(p_{i,x}(I(y))) dy \quad (5)$$

In the LGDF model, the Gaussian density function was used for modeling the probabilities of intensities and it was assumed that the mean and variance of the spatial Gaussian distribution are variables [20]:

$$p_{i,x}(I(y)) = \frac{1}{\sqrt{2\pi} \sigma_i(x)} \exp\left(-\frac{(u_i(x) - I(y))^2}{2(\sigma_i(x))^2}\right) \quad (6)$$

where $u_i(x)$ $\sigma_i(x)$ and are the mean and variance of the Gaussian distribution of the spatial variables, respectively.

The existence of the Gaussian kernel function causes the following: if y is close to x , in this condition the Gaussian kernel value will be large and the contribution of intensity will be significant for energy efficiency. On the other hand, when y is farther than x , then the value of the Gaussian kernel function decreases sharply to zero, so, that the contribution of intensity $I(y)$ will be zero for the energy efficiency. For all the central points of x in the image Ω , the ultimate goal is to minimize the following Equation:

$$E_x^{LGDF} = \int_{\Omega} \left(\sum_{i=1}^N \int_{\Omega_i} -\omega(x - y) \log(p_{i,x}(I(y))) dy \right) dx \quad (7)$$

By using the Heaviside function (H) and the level set function for the foreground and background areas, the energy functional can be defined as follows [20]:

$$E_x^{LGDF}(\phi, u_1(x), u_2(x), \sigma_1^2(x), \sigma_2^2(x)) = - \int \omega(x - y) \log(p_{1,x}(I(y))) M_1(\phi(y)) dy - \int \omega(x - y) \log(p_{2,x}(I(y))) M_2(\phi(y)) dy \quad (8)$$

In order to control the zero-level set smooth and handing noise for (8), a curve length is defined as follows:

$$L(\phi) = \int |\nabla H(\phi(x))| dx = \int \delta(\phi(x)) |\nabla \phi(x)| dx \quad (9)$$

To determine the level set function and its stability, the adjustment statement can be used:

$$R_p(\phi) \triangleq \int_{\Omega} p(|\nabla \phi|) dx \quad (10)$$

where p is a potential function. A simple choice of the potential function for the regularization statement is $p(s) = s^2$. One of these functions is the single-well potential [21], which has a minimum point in $S=1$ and is defined as follows [21]:

$$p(\phi) = \int \frac{1}{2} (|\nabla \phi(x)| - 1)^2 dx \quad (11)$$

Consequently, by combining (8) to (10), the energy efficiency is presented as follows [20]:

$$E_x^{LGDF}(\phi, u_1(x), u_2(x), \sigma_1^2(x), \sigma_2^2(x)) = - \int \omega(x - y) \log(p_{1,x}(I(y))) M_1(\phi(y)) dy - \int \omega(x - y) \log(p_{2,x}(I(y))) M_2(\phi(y)) dy + \nu L(\phi) + \mu p(\phi) \quad (12)$$

where the mean and variance are defined as:

$$u_i(x) = \frac{\int \omega(x-y) I(y) M_i(\phi(y)) dy}{\int \omega(x-y) M_i(\phi(y)) dy} \quad (13)$$

$$\sigma_i(x)^2 = \frac{\int \omega(x-y) (u_i(x) - I(y))^2 M_i(\phi(y)) dy}{\int \omega(x-y) M_i(\phi(y)) dy} \quad (14)$$

A standard method for minimizing functional energy

relative to ϕ is the solution of the gradient flow equation $\frac{\partial \phi}{\partial t} = -\frac{\partial F}{\partial \phi}$, where $\frac{\partial F}{\partial \phi}$ is the Gâteaux derivative [22] of the energy functional. Consequently, in order to minimize energy, it is better to take the Gâteaux derivative from (12), since there is need for the first derivative of the first term, with the change of the integral order, the energy can be re-written as follows:

$$E_{\varepsilon}^{\text{LGDF}} = \lambda_1 \int \left(\int \omega(x-y) \left(\log(\sqrt{2\pi}) + \log(\sigma_1(x)) + \frac{(u_1(x)-I(y))^2}{2\sigma_1(x)^2} \right) dx \times H_{\varepsilon}(\phi(y)) dy + \lambda_2 \int \left(\int \omega(x-y) \left(\log(\sqrt{2\pi}) + \log(\sigma_2(x)) + \frac{(u_2(x)-I(y))^2}{2\sigma_2(x)^2} \right) dx \times (1 - H_{\varepsilon}(\phi(y))) dy \right) \quad (15)$$

Hence, the Gâteaux derivative of (15) will be:

$$\frac{\partial E}{\partial \phi} = \delta_{\varepsilon}(\phi)(e_1 - e_2) - \nu \delta_{\varepsilon}(\phi) \text{div} \left(\frac{\nabla \phi}{|\nabla \phi|} \right) - \mu \left(\nabla^2 \phi - \text{div} \left(\frac{\nabla \phi}{|\nabla \phi|} \right) \right) \quad (16)$$

where Heaviside function, Dirac delta function and e_i are defined as:

$$H_{\varepsilon}(Z) = \frac{1}{2} \left(1 + \frac{2}{\pi} \arctan \left(\frac{Z}{\varepsilon} \right) \right) \quad (17)$$

$$\delta_{\varepsilon}(Z) = \frac{1}{\pi} \cdot \frac{\varepsilon}{Z^2 + \varepsilon^2} \quad (18)$$

$$e_i = \int \omega(x-y) \left(\log(\sigma_i(x)) + \frac{(I(y)-u_i(x))^2}{2\sigma_i(x)^2} \right) \quad (19)$$

Eq. (16) can be solved numerically by using a finite difference method (FDM). An approximation of (16) can be discrete as follows:

$$\phi_{i,j}^{n+1} = \phi_{i,j}^n + \Delta t \cdot Q(\phi_{i,j}^n) \quad (20)$$

Where Δt is the time step and $Q(\phi_{i,j}^n)$ is an approximation of the right hand of (19). For more details about LGDF on LGDF, see [20].

III. FEATURE EXTRACTION

During the development of biometric algorithms for two-dimensional images, one of the most important aspects of these algorithms is their proper evaluation. Commonly the image database of the ear is very rare and limited. In this paper, to evaluate the proposed algorithm for measuring the length, width and external angle of the ear, the AMI [23] and SUT [24, 25] databases were used.

The database of AMI contains ear images by views from front, right, left, bottom and top. This study used 31 images with frontal view. All the color images in this database are of size 492×702. The SUT database has an orthogonal system about the analyzing of face surgery. The above-mentioned system involves a head-fixer structure that can be increase the accuracy of imaging and particularly causes the head lie in best position. The control of this position is accomplished by a pulley and a balancing weight that they

make the system lie in the best location. The orthogonal imaging system has many advantages in the analyzing of facial surgeries. One of these advantages is simultaneously capturing three images from three orthogonal directions. The other advantages of this system are easy to use in healthcare units, and preventing any shaking during imaging by using a head-fixer. All images of SUT database resized into 800×800 then we choose of ear area manually. The image size of ear area is approximately 200×100. Finally, the results of these two databases will be presented separately in the conclusion section.

In the active contour model based on LGDF, the choice of values for the constant parameters λ_1 and λ_2 plays a very important role in moving the initial level set function to the beloved object. Based on the choice made, there are two modes for moving the initial level set function:

- If $\lambda_1 > \lambda_2$: in this case, the initial contour had to move to the outside of the object.
- If $\lambda_1 < \lambda_2$: in this case, the initial contour had to move to the inside of the object.

The main purpose was to extract the outer boundaries of contour of the ear region, as shown in Fig. 3, hence the most appropriate selection was $\lambda_1 > \lambda_2$. Table. I presents all constant parameters in the active contour model based on LGDF for extraction of the ear area.

To move the initial contour (selected manually) toward the external edges of the ear area and the extraction of its contour, first the background of the image was estimated by using the morphological opening with a disk SE of radius 15 and then the first channel of negative space was subtracted from the image background, as shown in Fig. 5(c), the output of this process will serve as input image for the LGDF model. As preprocessing step, we made the background uniform. To make the background illumination more uniform, we created an approximation of the background as a separate image and then subtracted this approximation from original image. The opening operator has the effect of removing objects that cannot completely contain the structuring element. After extracting the contour of the ear area, to extract the key points, the Harris Corner Detector (HCD) [26], as shown in Fig. 4(c) and Fig. 5(e), should be applied to the extracted contour area. From the obtained points through the Harris Corner Detector, the coordinates of 4 points (A, B, C and D) were obtained as follows, as shown in Fig. 4(d) and Fig. 5(f):

$$\begin{cases} A_y = \min(Y) \\ A_x = X(\text{local}(A_y)) \\ \text{if } \text{numel}(A_x) > 1 \rightarrow A_x = \min(A_x) \end{cases} \quad (21)$$

$$\begin{cases} B_y = \max(Y) \\ B_x = X(\text{local}(B_y)) \\ \text{if } \text{numel}(B_x) > 1 \rightarrow B_x = \max(B_x) \end{cases} \quad (22)$$

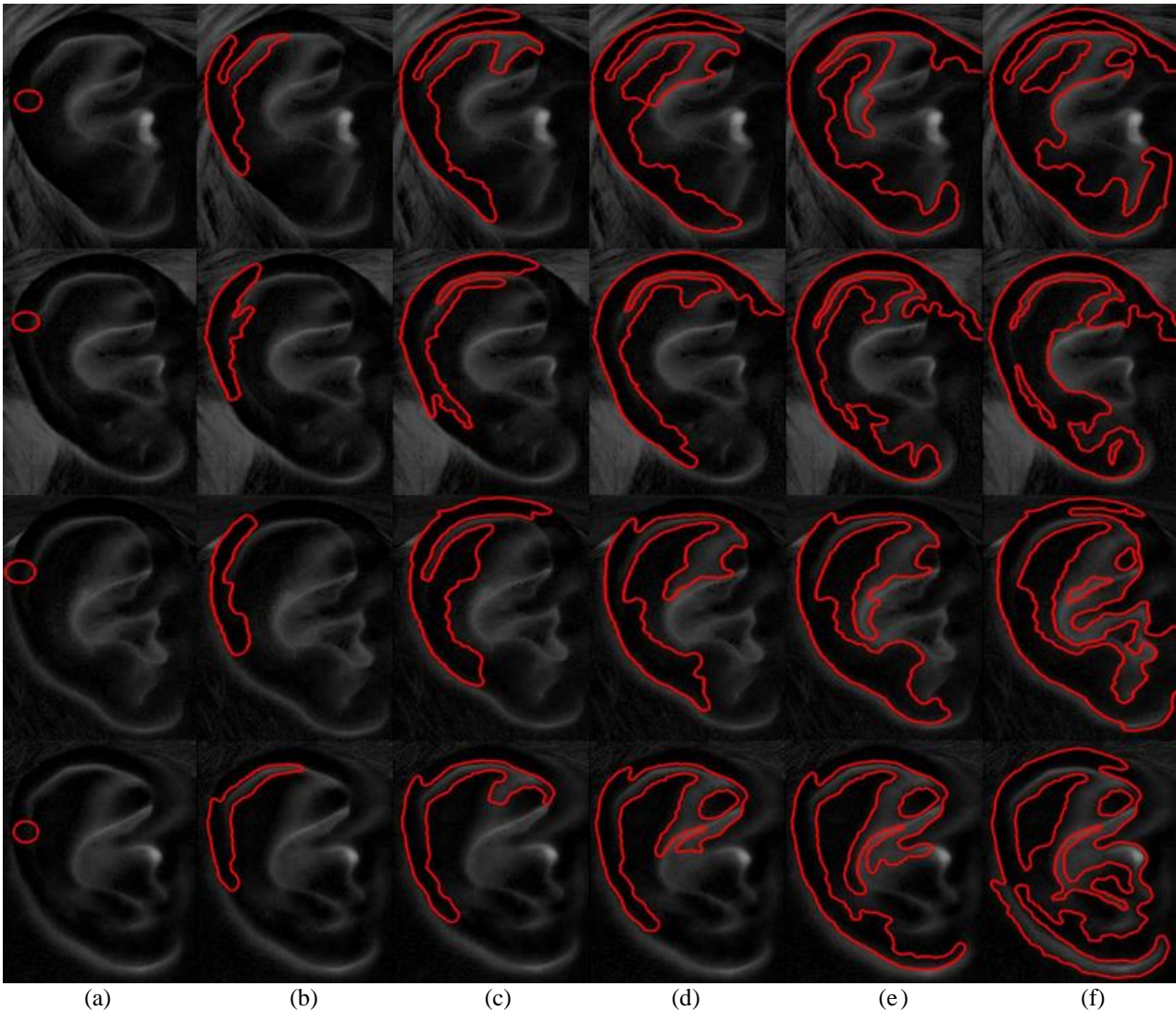


Fig. 3. An overview of contour extraction features of the ear area for AMI data. (a) Manual selection the initial surface on subtracted original image from estimated background using a disk SE of radius 15. (b) Iteration 400. (c) Iteration 800. (d) Iteration 1200. (e) Iteration 1600. (f) Iteration 2000.

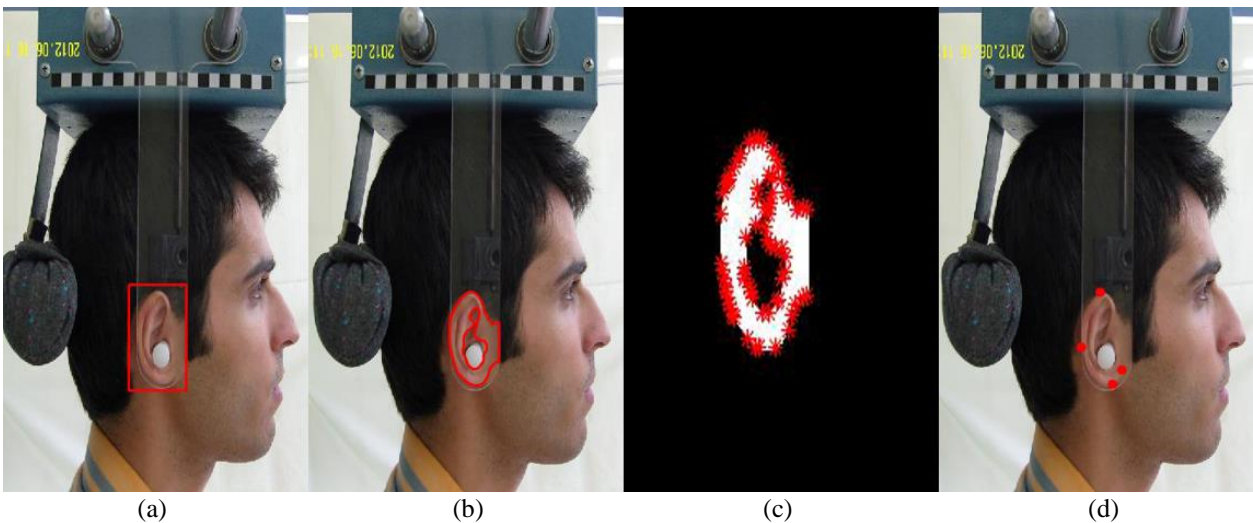


Fig. 4. A view of extraction of ear important landmarks on a sample data of SUT. (a) Manual selection the initial area, (b) Matching extracted contour over the original image, (c) Enforcement of Harris corner detector to extracted contour, (d) Detection the ear area important landmarks.

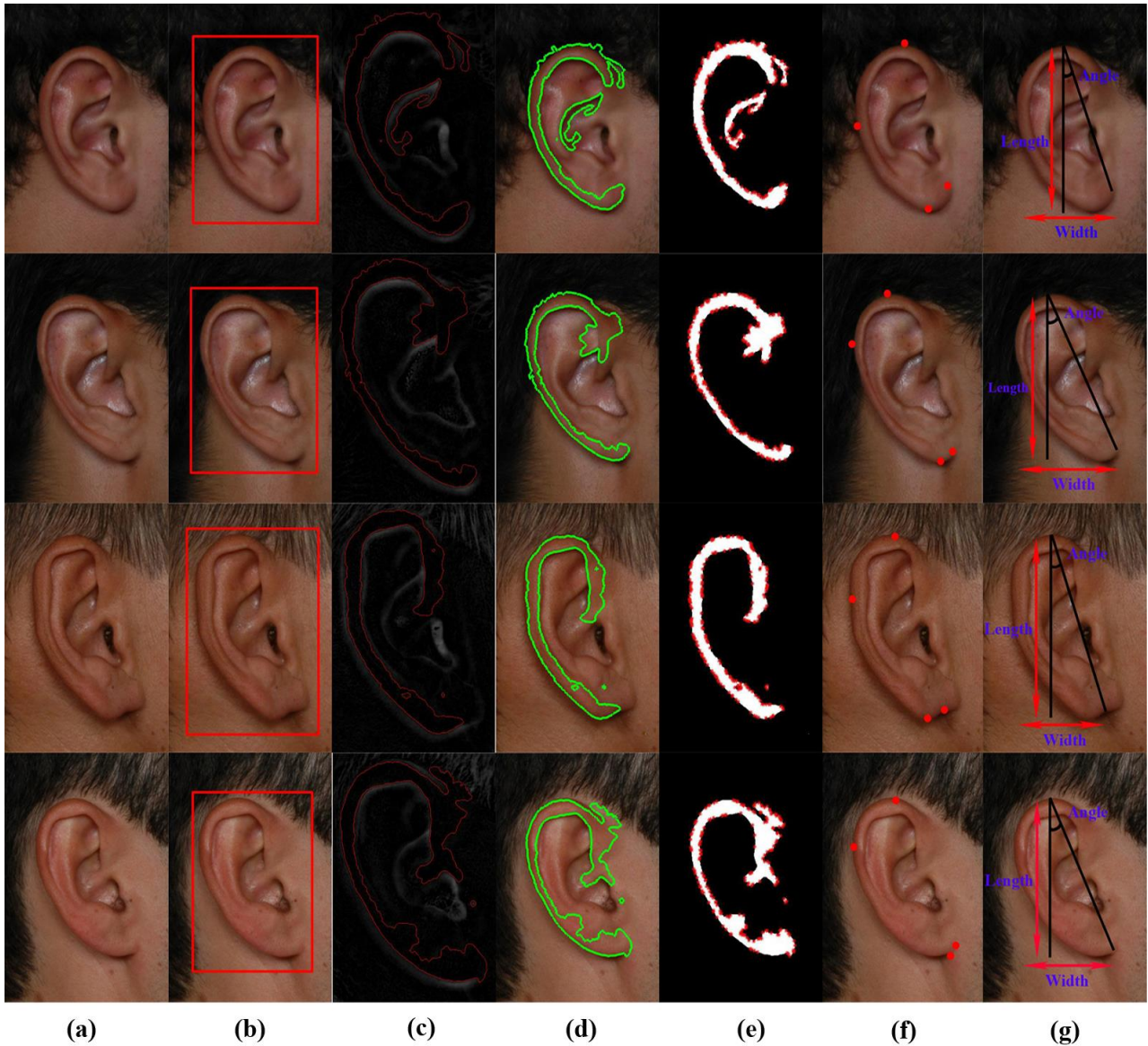


Fig. 5. Measurement of ear parameters for AMI data. (a) Original Image. (b) Manual selection the initial area. (c) Removing the image background and contour extraction. (d) Tracing of extracted contour on original image. (e) Apply of Harris Corner Detector to the extracted contour. (f) Extraction of ear important landmarks. (g) Parameter measurement.

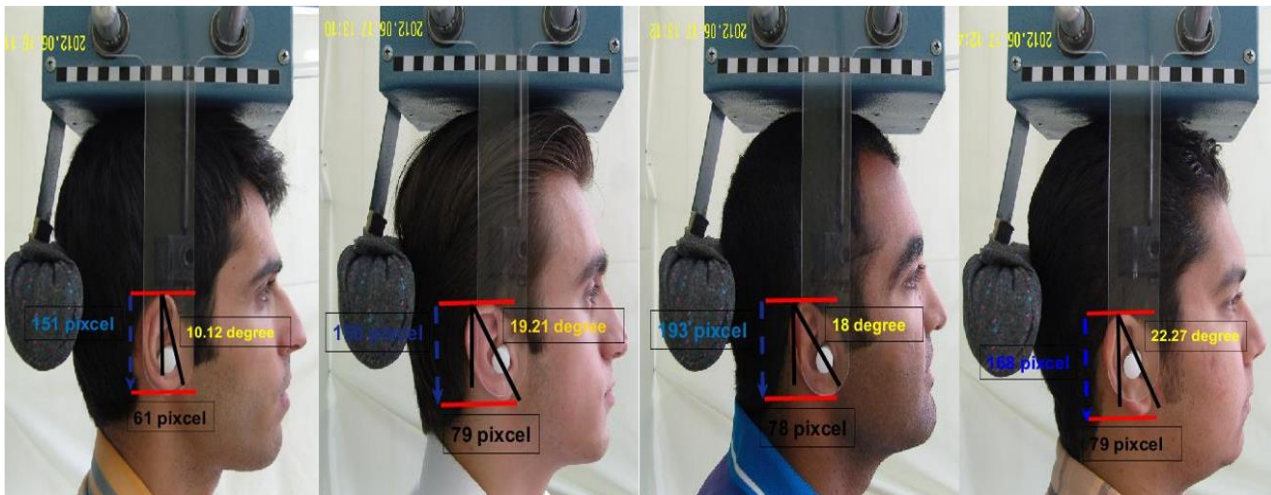


Fig. 6. An overview of measurement ear important parameters for analyzing Otoplasty surgery over the one sample of SUT data.

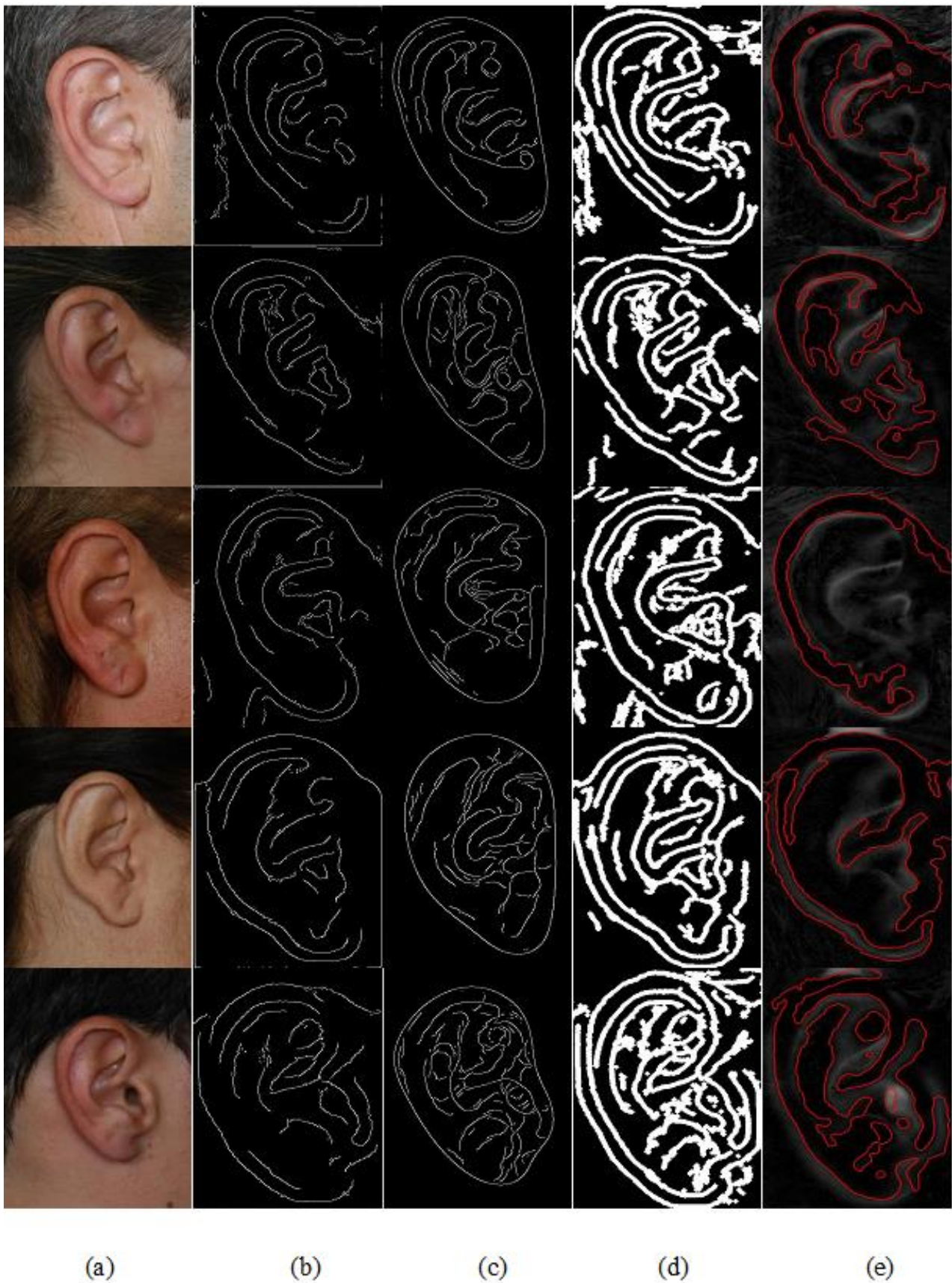


Fig. 7. The ear contour extraction. (Column 1) Original image. (Column 2) Ear contour extraction with [11]. (Column 3) Ear contour extraction with active contour model [10]. (Column 4) Ear contour extraction [12]. (Column 5) Ear contour extraction with the proposed algorithm.

obtained. The lobule portion of ear is located in one fourth quarter from end of ear. Therefore, the length of the ear is divided into 4 parts, and the coordinates of the desired point are obtained from the end part of 1/4 as follows:

$$\begin{cases} D_x = \max(X) \\ D_y = Y(\text{local}(D_x)) \\ \text{if } \text{numel}(D_y) > 1 \rightarrow D_y = \max(D_y) \end{cases} \quad (23)$$

After the extraction of landmarks from the ear region, in order to help the specialists in Otoplasty analysis, three important parameters, including: length, width and the external angle of the ear are measured.

TABLE I

VALUE OF PARAMETRS FOR THE LGDF MODEL.

| Interested area | λ_1 | λ_2 | Sigma | Iteration | Time step | μ |
|-----------------|-------------|-------------|-------|-----------|-----------|-------|
| Ear | 1.1 | 1.0 | 6.4 | 2000 | 0.1 | 1 |

IV. RESULTS AND DISCUSSION

The proposed algorithm is presented to measure the important parameters of the ear region including length, width and the external angle of the ear for Otoplasty surgery analysis. To quantitatively evaluate the proposed algorithm, 31 profile view images and 24 profile view images were randomly selected from the AMI (Fig. 5) and SUT (Fig. 6) databases, respectively. In our proposed algorithm, the input color images had a size of 492×702 and 800×800 pixels for AMI and SUT databases, respectively. The results obtained from the proposed algorithm were compared with those manually obtained. Manual measurement is a gold standard and represent the best measure available in reasonable conditions. This comparison is shown in Table. II and Table. III for AMI and SUT databases, respectively.

The tables show statistic information for the proposed method and manual measurement. The range of the length, width and external angle of the ear for AMI database are 337-518 (pixel), 154-307 (pixel) and 1.688°-28.193°, respectively. As well as, this measurement for SUT database are 129-187 (pixel), 62-86 (pixel) and 10.9°-29.4°, respectively. To determine the error and accuracy of the proposed algorithm, relations (24) were used:

$$E = \frac{|\varphi_m - \varphi_{pa}|}{\varphi_m} \times 100 \quad \text{and} \quad V = 100 - E \quad (24)$$

Where φ_m and φ_{pa} represent the manually measured angles and the angle measured with the proposed algorithm, respectively. E and V are indicating the error and accuracy of proposed algorithm, respectively. The average of these values for AMI and SUT databases have been shown in Table IV and Table V, respectively. Accuracy of the proposed method is %96.432, %97.423 and %85.546 for length, width and external angle of ear, respectively, on AMI database. As well as, these parameters have been shown in Table V for SUT database.

The proposed algorithm is a suitable method to extract contour of the ear region in presence of the image intensity inhomogeneity. In Fig. 7(b) and Fig. 7(d) [11,12], the filter mask is important to extract contour of the ear region. For this reason, this method will have different coefficients in the different images. The ear contour extraction with ACM is a manual method and depends on the user experience, as shown in Fig. 7(c) [10]. Canny Edge Detector [10-12] is not successful to extract contour in the images with non-uniform intensity. The proposed algorithm is able to solve this problem. As shown in Table IV and Table V, accuracy of the proposed algorithm is high for landmark detection including: superior point of the helical rim, midpoint of helix and lobule.

The proposed algorithm for the images is performed by an AMD A10-7400P system with a speed of 3.4 GHz, 4 GB RAM and the MATLAB programming language 2015.

TABLE II
THE MINIMUM, MAXIMUM, MEAN AND STANDARD DEVIATION VALUES FOR THE PROPOSED ALGORITHM AND MANUAL MEASUREMENT ON THE AMI DATABASE REGARDING 31 SAMPLES.

| Parameter | Proposed Algorithm | | | | Manual Measurement | | | |
|----------------|--------------------|--------|---------|--------|--------------------|-------|---------|--------|
| | Min | Max | Mean | SD | Min | Max | Mean | SD |
| Length (Pixel) | 337 | 518 | 431.156 | 40.861 | 306 | 580 | 462.875 | 52.949 |
| Width (Pixel) | 154 | 307 | 233.937 | 45.791 | 176 | 294 | 247.625 | 22.592 |
| External angle | 1.688 | 28.193 | 14.664 | 7.089 | 6.2 | 22.31 | 14.496 | 4.404 |

TABLE III
THE MINIMUM, MAXIMUM, MEAN AND STANDARD DEVIATION VALUES FOR THE PROPOSED ALGORITHM AND MANUAL MEASUREMENT ON THE SUT DATABASE REGARDING 24 SAMPLES.

| Parameter | Proposed Algorithm | | | | Manual Measurement | | | |
|----------------|--------------------|------|---------|--------|--------------------|------|---------|--------|
| | Min | Max | Mean | SD | Min | Max | Mean | SD |
| Length (Pixel) | 129 | 187 | 153.791 | 12.921 | 121 | 187 | 152.375 | 12.950 |
| Width (Pixel) | 62 | 86 | 74.958 | 7.135 | 60 | 88 | 74.50 | 7.223 |
| External angle | 10.9 | 29.4 | 19.541 | 4.587 | 10.9 | 29.4 | 19.575 | 4.753 |

TABLE IV
ACCURACY AND ERROR VALUES FOR THE PROPOSED ALGORITHM ON AMI DATABASE.

| Parameter | Ear Length | Ear Width | External angle of ear |
|-----------|------------|-----------|-----------------------|
| Accuracy | %96.432 | %97.423 | %85.546 |
| Error | 3.568 | 2.577 | 14.454 |

TABLE V
ACCURACY AND ERROR VALUES FOR THE PROPOSED ALGORITHM ON SUT DATABASE.

| Parameter | Ear Length | Ear Width | External angle of ear |
|-----------|------------|-----------|-----------------------|
| Accuracy | %98.381 | %97.37 | %87.864 |
| Error | 1.618 | 2.762 | 12.135 |

V. CONCLUSION

Nowadays, as a result of congenital problems, accidents, and beautiful facial structure, plastic surgeries have increased considerably in societies. In this case, one of the tasks of experts in this field is knowing the existence metrics in the facial areas before and after the surgery. Many peoples are unhappy with size and shape of their ears. Otoplasty surgery is used to reshape one or both ears and reposition the ears back into a natural position. The existence of software systems in the field of facial surgery analysis can help to surgeons in the before and after surgery to the process of improving and fast recognition of desired metrics. There is less research works in the field of Otoplasty surgery analysis using the image processing methods. In this paper, the analysis of ear anthropometry has been presented to assist ear surgery surgeons. The ear contour extraction is one of the most important part in the Otoplasty surgery analysis. The active contour model doesn't have suitable performance in the presence of shadow in the edge of ear area. Therefore, in this paper the contour extraction of the ear area has been done in the presence of shadow using the LGDF model, successfully. The main goal of this research is to determine important parameters of the ear area for the application of the analytical system in facial surgeries and Otoplasty Surgery. Therefore, in this study a new outlook based on image processing has been taken for Otoplasty surgery analysis. As well as, we have used the SUT database for analysis of ear area for the first time. This technique can be used as

part of the general system in the analysis of facial surgeries, specially, Otoplasty surgery. The speed and accuracy of the proposed method make it a distinct method among pattern recognition techniques. This research is very effective in developing simulation and evaluation systems for ear aesthetic surgery. This research is part of a system designed by our team for analysis of facial surgery. The designed system can be of great help to Otoplasty surgeons in improving the quality of the surgery and evaluation of ear area in before and after Otoplasty surgery. Three-dimensional measurement of the ear parameters using 3D models can be great help to Otoplasty surgery. We suggest a 3D models for ear anthropometry analysis including: length, width and external angle. Using the 3D models, the ear contour can be extracted with high accuracy. We suggest more landmarks detection in the ear area. The accuracy of Otoplasty surgery will increase with the more landmarks detection and precise anthropometry measurement.

REFERENCES

[1] Shamsi, Mousa, et al. "Automatic facial skin segmentation based on em algorithm under varying illumination." IEICE TRANSACTIONS on Information and Systems, vol. 91(5), pp. 1543-1551, 2008.
 [2] Handler, Ethan B., Tara Song, and Charles Shih. "Complications of otoplasty." Facial Plastic Surgery Clinics, vol. 21(4), pp. 653-662, 2013.

- [3] Stal, Samuel, Michael Klebuc, and Melvin Spira. "An algorithm for otoplasty." *Operative Techniques in Plastic and Reconstructive Surgery*, vol. 4(3), pp. 88-103, 1997.
- [4] Pulec, Jack L. "Facial plastic surgery clinic." *Ear, Nose & Throat Journal*, vol. 83(1), 2004.
- [5] Gutowski, Karol A. "Grabb & Smith's Plastic Surgery." *Plastic and Reconstructive Surgery*, vol. 120(2), 2007.
- [6] Bakhshali, Mohamad Amin, Mousa Shamsi, and Amir Golzarfar. "Facial color image enhancement for aesthetic surgery blepharoplasty." *IEEE Symposium on Industrial Electronics and Applications*, pp. 351-354, 2012.
- [7] Choi, Tae Joon, Jin Sik Burm, and Yung Ki Lee. "A Modified Closed Cartilage-Preserving Otoplasty Technique for Prominent Ear Correction." *Archives of Aesthetic Plastic Surgery*, vol. 22(2), pp.49-56, 2016.
- [8] Niamtu, Joe. "Cosmetic otoplasty." *The American Journal of Cosmetic Surgery*, vol. 28(4), pp.261-272, 2016.
- [9] Klockars, Tuomas, Antti Mäkitie, and Jorma Rautio. "Aesthetics of the auricle and its implications for otoplasty and auricular reconstruction." *International journal of pediatric otorhinolaryngology*, vol. 76(9), pp.1347-1350, 2012.
- [10] Anwar, Asmaa Sabet, Kareem Kamal A. Ghany, and Hesham Elmahdy. "Human ear recognition using geometrical features extraction." *Procedia Computer Science*, vol. 65, pp.529-537, 2015.
- [11] Mohanapriya, K., & Babu, M. M., "Ear Recognition by Feature Extraction Using Force Field Transformation," *International Journal of Engineering and Computer Science*, vol.6(3), pp. 20742-20750, 2017.
- [12] Omara, Ibrahim, et al. "A novel geometric feature extraction method for ear recognition." *Expert Systems with Applications*, vol. 65, pp.127-135, 2016.
- [13] Kumar, Ajay, and Chenye Wu. "Automated human identification using ear imaging." *Pattern Recognition*, vol. 45(3), pp.956-968, 2012.
- [14] Mayya, Ali Mahmoud, and M. Saii. "Human recognition based on ear shape images using PCA-Wavelets and different classification methods." *Med Devices Diagn Eng*, vol. 1(1), pp. 11-18, 2016.
- [15] Raghavendra, R., et al. "Improved ear verification after surgery-An approach based on collaborative representation of locally competitive features." *Pattern Recognition*, vol. 83, pp. 416-429, 2018.
- [16] Chowdhury, Debbrota Paul, et al. "Wavelet energy feature based source camera identification for ear biometric images." *Pattern Recognition Letters*, (2018).
- [17] Chatterjee, Amit, et al. "Ear biometrics recognition using laser biospeckled fringe projection profilometry." *Optics & Laser Technology*, vol. 112, pp. 368-378, 2019.
- [18] Gharsallah, Mohamed Ben, and Ezzedine Ben Braiek. "Automatic local Gaussian distribution fitting level set active contour for welding flaw extraction." *International Image Processing, Applications and Systems IEEE*, pp. 1-5, 2016.
- [19] Huang, Hailong, Xin Zuo, and Chao Huang. "Arbitrary initialization for Chan-Vese model." *Optik-International Journal for Light and Electron Optics*, vol. 125(18), pp.5257-5263, 2014.
- [20] Wang, Li, et al. "Active contours driven by local Gaussian distribution fitting energy." *Signal Processing*, vol. 89(12), pp. 2435-2447, 2009.
- [21] Li, Chunming, et al. "Distance regularized level set evolution and its application to image segmentation." *IEEE transactions on image processing*, vol. 19(12), pp.3243-3254, 2010.
- [22] L. C. Evans, Grad. Stud, "Math. Partial differential equations," vol. 37, 2000.
- [23] http://www.ctim.es/research_works/ami_ear_database/.
- [24] Bakhshali, Mohamad Amin, and Mousa Shamsi. "Estimating facial angles using Radon transform." *Turkish Journal of Electrical Engineering & Computer Sciences*, vol. 23(3), pp. 804-812, 2015.
- [25] Bakhshali, Mohamad Amin, Mousa, Shamsi and Mohammad, Sadeghi, "Evaluation of facial soft tissue parameters for Northwestern students in Iran". *Journal of Craniomaxillofacial Research*, vol. 2(1-2), pp. 78-82, 2015.
- [26] Peng, Wu, et al. "Harris scale invariant corner detection algorithm based on the significant region." *International Journal of Signal Processing, Image Processing and Pattern Recognition*, vol. 9(3) pp.413-420, 2016.

تخمین پارامترهای گوش به منظور کاربرد در آنالیز جراحی اتوپلاستی

علی فهمی جعفرقلخانلو^۱، موسی شمسی^{۲*}

۱- دانشکده مهندسی پزشکی، گروه بیوالکتریک، دانشگاه صنعتی سهند تبریز، تبریز، ایران.

۲- دانشکده مهندسی پزشکی، گروه بیوالکتریک، دانشگاه صنعتی سهند تبریز، تبریز، ایران.

^۱a_fahmi@sut.ac.ir, ^۲*shamsi@sut.ac.ir

* نشانی نویسنده مسئول: موسی شمسی، تبریز، شهر جدید سهند، دانشگاه صنعتی سهند تبریز، دانشکده مهندسی پزشکی، گروه بیوالکتریک، کد پستی:

چکیده- آنالیز تصاویر رنگی چهره به دلیل کاربردهای فراوان آن در جراحی‌های چهره دارای اهمیت زیادی است. وجود ابزارهای سخت‌افزاری و نرم‌افزارهای شبیه‌ساز، کمک شایانی را می‌توانند به متخصصین جراحی‌های چهره در آنالیز سفالومتری چهره در قبل و بعد عمل جراحی داشته باشند. در این مقاله، به منظور استخراج ناحیه‌ی گوش از مدل کانتور فعال مبتنی بر تبدیل گاو سینم کانی (LGDF) استفاده شده است. مدل معرفی شده یک مدل مبتنی بر ناحیه در مدل کانتور فعال بوده، که برخلاف سایر مدل‌ها نظیر چان-ویس به غیریکنواختی شدت مکانی تصویر حساس نیست. به منظور آنالیز آنتروپومتری گوش جهت کاربرد در جراحی اتوپلاستی، ابتدا کانتور ناحیه‌ی گوش را با استفاده از مدل LGDF استخراج کرده، سپس با آشکارسازی ۴ لندمارک، پارامترهای گوش شامل طول، عرض و زاویه‌ی خارجی گوش اندازه‌گیری شده‌اند. جهت ارزیابی الگوریتم پیشنهادی از دو پایگاه داده‌ی AMI و دانشگاه صنعتی سهند تبریز (SUT) استفاده شده است. دقت الگوریتم ارائه شده برای اندازه‌گیری پارامترهای طول، عرض و زاویه‌ی خارجی گوش بر روی تصاویر پایگاه داده‌ی AMI به ترتیب ۹۶/۴۳۲٪، ۹۷/۴۲۲٪ و ۸۵/۵۴۶٪ و بر روی تصاویر پایگاه داده‌ی SUT به ترتیب ۹۸/۲۸۱٪، ۹۷/۲۳۷٪ و ۸۷/۸۶۴٪ است. نتایج به دست آمده نشان می‌دهند که از نتایج این آنالیز می‌توان به عنوان یک سیستم نرم‌افزاری در شبیه‌سازهای جراحی چهره و اتوپلاستی استفاده کرد.

واژه‌های کلیدی: آنالیز آنتروپومتری گوش، آنالیز تصاویر رنگی، آنالیز جراحی چهره، آنالیز جراحی اتوپلاستی، مدل کانتور فعال.